NASA TECHNICAL NOTE

NASA TN D-7572

NASA TN D-7572

# ANALYSIS OF THE THREE-POINT-BEND TEST FOR MATERIALS WITH UNEQUAL TENSION AND COMPRESSION PROPERTIES

*by Christos C. Chamis*

*Lewis Research Center*
*Cleveland, Ohio 44135*

NATIONAL AERONAUTICS AND SPACE ADMINISTRATION • WASHINGTON, D. C. • MARCH 1974

| 1. Report No. | 2. Government Accession No. | 3. Recipient's Catalog No. |
|---|---|---|
| NASA TN D-7572 | | |

| 4. Title and Subtitle | 5. Report Date |
|---|---|
| ANALYSIS OF THE THREE-POINT-BEND TEST FOR MATERIALS WITH UNEQUAL TENSION AND COMPRESSION PROPERTIES | MARCH 1974 |
| | 6. Performing Organization Code |
| 7. Author(s) | 8. Performing Organization Report No. |
| Christos C. Chamis | E-7544 |
| | 10. Work Unit No. |
| 9. Performing Organization Name and Address | 501-22 |
| Lewis Research Center<br>National Aeronautics and Space Administration<br>Cleveland, Ohio 44135 | 11. Contract or Grant No. |
| | 13. Type of Report and Period Covered |
| 12. Sponsoring Agency Name and Address | Technical Note |
| National Aeronautics and Space Administration<br>Washington, D.C. 20546 | 14. Sponsoring Agency Code |

15. Supplementary Notes

16. Abstract

An analysis capability is described for the three-point-bend test applicable to materials of linear but unequal tensile and compressive stress-strain relations. The capability consists of numerous equations of simple form and their graphical representation. Procedures are described to examine the local stress concentrations and failure modes initiation. Examples are given to illustrate the usefulness and ease of application of the capability. Comparisons are made with materials which have equal tensile and compressive properties. The results indicate possible underestimates for flexural modulus or strength ranging from 25 to 50 percent greater than values predicted when accounting for unequal properties. The capability can also be used to reduce test data from three-point-bending tests, extract material properties useful in design from these test data, select test specimen dimensions, and size structural members.

| 17. Key Words (Suggested by Author(s)) | 18. Distribution Statement |
|---|---|
| Bending test; Unequal tension-compression material properties; Testing; Stress-analysis; Stress concentrations; Structural-analysis; Design; Structural resins; Fiber composites | Unclassified - unlimited<br>Cat. 32 |

| 19. Security Classif. (of this report) | 20. Security Classif. (of this page) | 21. No. of Pages | 22. Price* |
|---|---|---|---|
| Unclassified | Unclassified | 33 | $3.00 |

* For sale by the National Technical Information Service, Springfield, Virginia 22151

# ANALYSIS OF THE THREE-POINT-BEND TEST FOR MATERIALS WITH UNEQUAL TENSION AND COMPRESSION PROPERTIES

by Christos C. Chamis

Lewis Research Center

## SUMMARY

An analysis capability is described for the three-point-bend test applicable to materials of linear but unequal tensile and compressive stress-strain relations. The capability provides numerous equations of simple form and their graphical representation. The various equations are derived using linear structural mechanics principles. Procedures are described for determining the local stress concentration in the vicinity of the load point and the failure mode at the critical stress location.

Examples are given to illustrate the usefulness and ease of applicability. The functional behavior of the equations is described graphically. This is done to expedite the analysis and to illustrate the influence of material properties and geometric parameters on properties such as: maximum deflection, maximum tensile (compressive) stress, maximum shear stress, flexural modulus, shear modulus, and local stress concentrations.

Comparisons are made with values obtained when the material is considered to have equal tensile and compressive mechanical properties. Some typical results from these comparisons follow: The maximum bending deflection and stress can be underestimated by 25 percent or more. The flexural modulus can be underestimated by 35 percent, and the shear modulus by 25 percent. The horizontal shear stress can be underestimated by 15 percent in the vicinity of local stress concentrations. No corrections are required for the maximum bending stresses and deflection when the length-to-depth ratio is 20 or greater. Failure initiates on the tensile side when the material's compressive strength is equal to or greater than its tensile strength.

The capability can also be used to reduce test data from three-point-bend tests, extract material properties useful in design from these test data, select test specimen dimensions, and size structural members.

## INTRODUCTION

Structural resins are used extensively as matrices in advanced fiber composites. These resins have moduli and strengths that are different in tension and compression. Typical ranges of ratios are, for the compression-modulus to tensile-modulus ratio, 1.0 to 1.5 and, for the compressive-strength to tensile strength ratio, 1.5 to 2.0.

Structural resins are generally characterized by means of the three-point-bend test. The test data are reduced using simple beam formulas that do not account for different tensile and compressive properties. The reduced data can be in considerable error depending on the magnitude of the difference between the tensile and compressive properties.

There are several good reasons why the three-point-bend test is used extensively in material characterization: economy, simplicity of specimen preparation and testing, ease of adaptability to enviromental testing, suitability for cyclic loading and fatigue testing, convenience for fracture toughness studies, and the availability of well documented simple formulas for analyzing materials having equal tension and compression properties (refs. 1 to 4). Another important reason is that the three-point-bend test is a simple way to subject a specimen to tension, compression, and shear simultaneously. In this sense, a three-point-bend test provides a direct measure of the structural integrity of the material.

Available simple beam formulas are used for analysis because no comparable formulas are available which account for different tensile and compressive mechanical properties. Therefore, an investigation was performed to derive all the equations needed for the analysis and test data reduction of three-point-bend test for materials with unequal tensile and compressive mechanical properties. The specific objectives were the

(1) Derivation of all the equations needed in the form of simple formulas

(2) Investigation of the stress concentration effects in the vicinity of the load point

(3) Examination of failure stress and failure initiation.

The governing equations were derived using well known linear structural mechanics principles. Symbols are defined when they first appear and are also compiled in appendix A for your convenience. The equations are described in the main text where several examples are given to illustrate their simplicity and usefulness. The detailed derivations are presented in appendix B. Although the terms "bending" and "flexural" are used interchangeably, herein, I use only flexural for consistency. Analogous equations can be derived for the four-point-bend test by following the procedure used in appendix B.

## THEORY AND USEFUL EQUATIONS

### Theoretical Background

Closed form equations for analyzing or reducing data from a three-point-bend test (fig. 1) are described herein. The equations are for shift of the neutral plane (zero bending stress plane), maximumum bending deflection, flexural (bending) modulus, shear modulus, maximum bending stress, and maximum shear stress. Only the final equations are given herein. The detailed derivations are given in appendix B.

The equations are derived following the procedure used in classical beam theory but accounting for different moduli in tension and compression. Briefly, classical beam theory is based on the elastomechanics concepts of force equilibrium, stress-strain relations, strain displacement relations, and the conservation of elastic strain energy. In the present development, it is assumed that both the stress-strain and strain displacement relations are linear.

The following equations and relations were used to develop the theory presented herein (refer to fig. 1). The force equilibrium equation at a point (x, z) in the beam is given by

$$\frac{d\sigma}{dx} - \frac{d\tau}{dz} = 0 \tag{1}$$

where $\sigma$ and $\tau$ denote normal and shear stress, respectively. The resultant force at a section x is given by

$$\int_{-h_b}^{0} \sigma_T dz + \int_{0}^{h_t} \sigma_C dz = 0 \tag{2}$$

where $h_b$ is measured from the neutral plane to the bottom of the beam and $h_t$ to the top (fig. 1(b)). The subscripts T and C denote tension and compression, respectively. The resultant moment at a section x is given by

$$M = b \int_{-h_b}^{0} \sigma_T z dz + b \int_{0}^{h_t} \sigma_C z dz \tag{3}$$

where b is the beam width. The linear stress strain relations are given by

$$\epsilon_T = E_T \sigma_T \qquad \epsilon_C = E_C \sigma_C \qquad \tau = G\gamma \tag{4}$$

where $\epsilon$ and $\gamma$ denote normal and shear strain, respectively, and E and G denote normal and shear modulus, respectively.

The linear strain displacement relation at a point z is given by

$$\epsilon = -z \frac{d^2w}{dx^2} \tag{5}$$

where w is the bending deflection and $(d^2/dx^2)$ denotes the second derivative.

The details on how equations (1) to (5) were used to derive the governing equations of interest herein are given in appendix B. The property and governing equations are briefly described in subsequent sections. The governing equations are used to illustrate the effect of the modular ratio $E_T/E_C$ on the property under discussion.

## Neutral Plane Location and Bending Stiffness

The location of the neutral plane (plane of zero bending stress, fig. 1(b)) is given by

$$\frac{h_t}{h_b} = \left(\frac{E_T}{E_C}\right)^{1/2} \tag{6}$$

$$h_b = \frac{h}{\left[1 + \left(\frac{E_T}{E_C}\right)^{1/2}\right]} \tag{7}$$

where h is the beam thickness (fig. 1).

The shift of neutral plane as a function of modular ratio $E_T/E_C$ is presented graphically in figure 2. As can be seen in this figure, the neutral plane shift exceeds 10 percent when the modular ratio is less than 0.8 or greater than 1.2. It is useful to note from equation (7) and figure 2 that the neutral plane shifts towards the higher-modulus material.

The bending stiffness, also known as bending rigidity or flexural rigidity, is given by

$$D = \frac{b}{3}\left(h_b^3 E_T + h_t^3 E_C\right) \tag{8}$$

where D denotes the bending stiffness. The effects of the modular ratio on the bending stiffness will be illustrated later.

Equation (8) can also be given as

$$D = \frac{1}{3} bhh_b^2 E_T \tag{8a}$$

or

$$D = \frac{1}{3} bhh_t^2 E_C \tag{8b}$$

or

$$D = \frac{bh^3 E_T}{3\left[1 + \left(\frac{E_T}{E_C}\right)^{1/2}\right]^2} \tag{8c}$$

It can be readily verified by inspection that equations (8) reduce to the well known expression $Ebh^3/12$ when the modular ratio equals one.

Equation (8c) indicates that when the tensile modulus only is used to calculate bending deflections, the deflection will be underestimated if $E_T/E_C < 1.0$ and overestimated if $E_T/E_C > 1.0$.

## Maximum Flexural Deflection

The equation for computing the maximum bending deflection (deflection at midpoint) is given by

$$w_{max} = \frac{Pl^3}{48D}\left[1 + 1.6\, bh_b^2 h\, \frac{E_T^2}{GD}\left(\frac{h_b}{l}\right)^2\right] \tag{9}$$

where P is the load, $l$ is the length, and G is the shear modulus.

The shear modulus for a material with different tensile and compressive moduli is given by (see appendix B)

$$G = \frac{E_T}{\left[1 + 2\nu_T + \left(\frac{E_T}{E_C}\right)\right]} \tag{10}$$

where $\nu_T$ is the Poisson's ratio measured on a tensile test.

The influence of the modular ratio on the flexural deflection is shown in figure 3 where the variable $w_{max}/w_{Fmax}$ is plotted against $l/h$ for various $E_T/E_C$. The variable $w_{Fmax}$ is the flexural deflection for the case where $E_T/E_C = 1.0$ and for no shear contribution. It is given by

$$w_{Fmax} = \frac{Pl^3}{4bh^3E_T} \tag{11}$$

Two points are worthy of note in figure 3:

(1) The modular ratio has significant influence on the flexural deflection. The simple formula (eq. (11)) underestimates the flexural deflection by 25 percent when $E_T/E_C = 1.5$ and overestimates it by 25 percent when $E_T/E_C = 0.5$. These observations were anticipated from the discussion following equation (8c).

(2) The length-to-depth ratio $l/h$ has negligible effect on the flexural deflection when $l/h > 10$ in the range of modular ratio $0.5 \leq E_T/E_C \leq 2.0$. This is an important observation because the researcher does not have to be overly concerned about the specimen length so long as it has a length-to-depth ratio greater than 10.

## Bending and Shear Moduli

The apparent flexural modulus from a three-point-bend test is obtained by solving equation (11) for E. The result is

$$E_F = \frac{Pl^3}{4bh^3w_{Fmax}} \tag{12}$$

where $E_F$ is the apparent flexural modulus and $w_{Fmax}$ is the measured deflection under the load. Equation (12) assumes that the neutral plane coincides with the midplane of the beam.

The error introduced in equation (12) when $E_T/E_C \neq 1.0$ may be calculated by using $w_{Fmax}$ from equation (9) in equation (12). This is illustrated in figure 4 where the nondimensional variable $E_F/E_T$ is plotted against the modular ratio for $l/h = 10$ and 40 (flexural modulus from deflection curves). As can be observed from figure 4, the influence of the modular ratio on the apparent flexural modulus is considerable.

The flexural modulus may also be estimated by the approximate relation, which is derived by averaging the stiffnesses (see appendix B)

$$E_F \approx \left(\frac{h_b}{h_t}\right)E_T = \sqrt{E_T E_C} \tag{13}$$

where $E_F$ denotes the approximate flexural modulus. The ratio $E_F/E_T$ is plotted against $E_T/E_C$ in the figure 4 curve labeled "flexural modulus" (approximate). As can be seen in figure 4, the approximate flexural modulus is a good approximation (less than 5 percent error) when $0.75 \leq E_T/E_C \leq 2.0$.

The effects of the modular ratio on the shear modulus are obtained from equation (10). The shear modulus from equation (10) nondimensionalized with respect $G_{ISO}$ is plotted against $E_T/E_C$ in figure 5, where $G_{ISO}$ is the shear modulus of an isotropic material and is given by

$$G_{ISO} = \frac{E}{2(1 + \nu)} \tag{14}$$

As can be seen in figure 5, the modular ratio $E_T/E_C$ has considerable effect (as high as 25 percent) on the shear modulus.

The conclusions to be made from the previous discussion and the curves in figures 4 and 5 are

(1) Modular ratio $E_T/E_C$ has significant influence on the flexural and shear moduli (could be as high as 35 and 25 percent, respectively, for $0.5 \leq E_T/E_C \leq 2.0$)

(2) The length-to-depth ratio $l/h$ has insignificant effects on the flexural modulus

(3) The flexural modulus may be approximated sufficiently closely using a simple equation.

## Maximum Flexural and Shear Stresses

The maximum flexural tensile stress occurs at $x = l/2$ and $z = -h_b$ (fig. 1(b)). The equation to predict this stress is given by

$$\sigma_{Tmax} = P\ell h_b \frac{E_T}{4D} \tag{15}$$

or

$$\sigma_{Tmax} = \frac{3P}{4bh_b}\left(\frac{\ell}{h}\right) \tag{15a}$$

The maximum bending compressive stress occurs at $x = \ell/2$ and $z = h_t$ (fig. 1(b)). The equation to predict this stress is given by

$$\sigma_{Cmax} = -P\ell h_t \frac{E_C}{4D} \tag{16}$$

or

$$\sigma_{Cmax} = \frac{-3P}{4bh_t}\left(\frac{\ell}{h}\right) \tag{16a}$$

Letting $h_b = h/2$ in equation (15a) and $h_t = h/2$ in equation (16a) result in

$$\sigma_{max} = 1.5 \frac{P\ell}{bh^2} \tag{17}$$

which is the equation given for a material with equal moduli in tension and compression.

Nondimensionalizing equation (15a) with respect to equation (17) results in

$$\frac{\sigma_{Tmax}}{\sigma_{max}} = \frac{h}{2h_b} \tag{18}$$

The corresponding result for $\sigma_{Cmax}$ is given by

$$\frac{\sigma_{Cmax}}{\sigma_{max}} = \frac{h}{2h_t} \tag{19}$$

Equations (18) and (19) indicate that the maximum flexural stress (tensile or compressive) occurs on the extreme fibers of the stiffer side. The graphical representation of

$\sigma_{Tmax}$ and $\sigma_{Cmax}$ against $E_T/E_C$ is shown in figure 6, which shows that the corrections to the maximum stresses can be as much as 20 percent.

Two more useful stress ratios are obtained by dividing equation (15a) by equation (16a) and then using equation (6). The results are

$$\frac{\sigma_{Tmax}}{\sigma_{Cmax}} = \frac{h_t}{h_b} = \left(\frac{E_T}{E_C}\right)^{1/2} \tag{20}$$

Equation (20) indicates that the ratio of the maximum stresses varies as the square root of the ratio of their respective moduli.

The maximum shear stress is given by the equation

$$\tau_{xzmax} = 0.75\,\frac{P}{bh} \tag{21}$$

which is the same as that given for a material with $E_T/E_C = 1.0$. The reason for this condition is that the shear stress equals zero at the top and bottom surfaces of the beam. These boundary conditions can only be satisfied by a parabolic variation of the shear stress through the beam thickness. However, the plane of maximum shear stress is at $z = 0$ and depends on the modular ratio. This dependence is illustrated graphically in figure 2.

The important points to be noted from the previous discussion are

(1) Simple relations for various stress ratios exist

(2) The stress ratio $\sigma_{Tmax}/\sigma_{Cmax}$ varies as the square root of the modular ratio and attains its largest magnitude on the extreme fibers of the stiffer side

(3) The correction to either $\sigma_{Tmax}$ or $\sigma_{Cmax}$ can be as large as 25 percent when compared with a material with equal moduli

(4) The magnitude of the maximum shear stress is independent of the modular ratio. However, the plane at which the maximum shear stress occurs depends on the modular ratio.

## STRESSES AND DISPLACEMENTS IN THE VICINITY OF THE LOAD

The equations described previously predict the stresses quite accurately at a distance one-half the thickness away from the load application point. In the vicinity of the load these equations need additional corrections. In this vicinity (point A, fig. 1(b) both x and z direction stresses have the same sign, and equations with equal moduli are applicable.

In reference 5 approximate equations are presented for a material with equal moduli for tension and compression. The equations from reference 5 are presented herein and discussed briefly to illustrate the effects of stress concentration.

The stress in the x-direction in the section under the load is given by (see fig. 7(d))

$$\sigma_x = -\frac{3Pl}{bh^2}\left\{\left[1 - \frac{2}{\pi}\left(\frac{h}{l}\right)\right]\left(\frac{z}{h}\right) - \frac{1}{3\pi}\left(\frac{h}{l}\right) - \frac{2}{3\pi}\left(\frac{h}{l}\right)\left[\frac{3}{5}\left(\frac{z}{h}\right) - 4\left(\frac{z}{h}\right)^3\right]\right\} \tag{22}$$

where

$$-\frac{h}{2} < z \leq \frac{h}{2} \tag{23}$$

and for $z = -(h/2)$

$$\sigma_x = \frac{3Pl}{2bh^2}\left[1 - 0.177\left(\frac{h}{l}\right)\right] \tag{24}$$

Both equations (22) and (24) indicate that the stress concentration correction to $\sigma_x$ is insignificant and becomes negligible as $l/h > 10$. A graphical representation of the local stress concentration contributions to $\sigma_x$ through the beam thickness is shown in figure 7(a). Note that the correction decreases both the tensile and compressive stress values predicted by the beam formula. Stated differently, the beam formula slightly overpredicts the flexural stresses.

The stress in the z-direction (fig. 7(d)) at the section under the load is given by

$$\sigma_z = \frac{P}{\pi bh}\left\{1 + 2\left[2\left(\frac{z}{h}\right)^3 - \frac{3}{2}\left(\frac{z}{h}\right)\right] - \frac{4}{1 - 2\left(\frac{z}{h}\right)}\right\} \tag{25}$$

where

$$-\frac{h}{2} \leq z < \frac{h}{2} \tag{26}$$

and

$$\sigma_z \to -\infty \quad \text{as} \quad z \to \frac{h}{2} \tag{27}$$

Note that the condition indicated by equation (27) is typical of elastic solutions near singularities. However, $\sigma_z$ will produce permanent damage locally when $\sigma_z$ has exceeded the compressive strength of the material.

The graphical representation of equation (25) is shown in figure 7(b), where the $\sigma_z$ variation through the thickness is plotted. As can be seen in figure 7(c), $\sigma_z$ decays very rapidly away from the load point.

The shear stress variation through the beam thickness at a section in the vicinity of the load (fig. 7(d)) is shown in figure 7(c). This figure was generated from data given in reference 5 (p. 105). The interrupted portion of this curve indicates the lack of data in that region. The maximum shear stress occurs at $z = h/4$ (fig. 7(c)) with an approximate value of

$$\tau_{xz} \approx 0.86 \frac{P}{bh} \tag{28}$$

The maximum shear stress from the simple beam formula is given by equation (21). The ratio of equation (28) to equation (21) is

$$\frac{\tau_{xz\ \text{local}}}{\tau_{xz\ \text{simple-beam}}} = \frac{0.86}{0.75} = 1.15 \tag{29}$$

This leads to the conclusion that the maximum shear stress can be about 15 percent greater than that obtained by means of the simple beam theory and that it occurs at about $z = h/4$.

The maximum deflection is also affected by the stress concentration in the vicinity of the load. For a material with equal moduli in both tension and compression, the equation from reference 5 (p. 107) is

$$w = \frac{P\ell^3}{4bh^3E}\left\{1 + 2\left(\frac{h}{\ell}\right)^2\left[\frac{3}{4}\left(\frac{E}{G}\right) - \frac{3}{10} - \frac{3}{4}\nu\right] - 0.84\left(\frac{h}{\ell}\right)^3\right\} \tag{30}$$

For a material with equal moduli, in both tension and compression, equation (9) reduces to

$$w = \frac{P\ell^3}{4bh^3E}\left[1 + 1.2\left(\frac{h}{\ell}\right)^2\left(\frac{E}{G}\right)\right] \tag{31}$$

Assuming $\nu = 0.4$ and using the isotropic relation $E = 2(1 + \nu)G$, the middle term in equation (30) becomes $3.00(h/\ell)^2$. The corresponding term in equation (31) is $3.36(h/\ell)^2$. The conclusion from this exercise is that equation (31) and, therefore, equation (9), overestimates the shear contribution to the maximum deflection. It can be verified by direct substitution that both shear and local stress contribute less than 1 percent to the maximum deflection when $(\ell/h)$ is 20 or greater.

The previous discussion leads to the following conclusions:

(1) The local stress concentration has negligible effect on the bending stresses and bending deflections predicted by simple beam formulas when $\ell/h$ is equal to or greater than 20.

(2) The through-the-thickness normal stress $\sigma_z$ is very high in the immediate vicinity of the load point. It decreases very rapidly as the distance away from the load point increases.

(3) The local stress concentration contributes about 15 percent to the maximum shear stress predicted by the simple beam formula, and it occurs at about the top one-fourth point.

## EFFECTS OF STRESS CONCENTRATION ON THE SPECIMEN FAILURE STRESS

The effects of the local stress concentration on the specimen failure stress are considered in this section. The stress state at point A (fig. 1(a)) is biaxial compression. An equation describing the combined-stress-state failure envelope for a material with different strength in tension and compression is given by (ref. 6 with $K_{\ell 12}$ and $K_{\ell 12\alpha\beta}$ replaced by $K_{xz\alpha\beta}$)

$$F(\sigma_x, \sigma_z, \sigma_{xz}) = 1 - \left[\left(\frac{\sigma_{x\alpha}}{S_{x\alpha}}\right)^2 + \left(\frac{\sigma_{z\beta}}{S_{z\beta}}\right)^2 + \left(\frac{\sigma_{xz}}{S_{xz}}\right)^2 - K_{xz\alpha\beta}\frac{\sigma_{x\alpha}}{S_{x\alpha}}\frac{\sigma_{z\beta}}{S_{x\beta}}\right] \tag{32}$$

where $F$ is the combined stress failure function, $\sigma$ is the stress due to load, $S$ is the unaxial failure strength, $K$ depends on the elastic constants of the material and is unity

for isotropic materials, the subscripts x and z denote direction, and the subscripts $\alpha$ and $\beta$ denote tension or compression.

The envelope described by equation (32) is shown in figure 8 for a material with room-temperature properties representative of epoxy resins and a value of $K_{xz\alpha\beta} = 1.0$. Combined or uniaxial stress states causing failure are represented by points on the failure envelope curve in figure 8.

Applying this information to the failure stress of a three-point-bend test and recalling the local stress concentration effects on the flexural stresses from the previous section lead to the following conclusion: Failure will initiate on the tension side of a three-point-bend test specimen that is made from materials with compressive strength equal to or greater than the tensile strength.

The preceding conclusion is obvious from both intuition and figure 8 for the case when the compressive strength is greater than the tensile. The case of equal strengths is a little more subtle and can be shown by the following procedure:

(1) Assume a representative value of $l/h$. Herein we assume $l/h = 20$.

(2) Assume the specimen fails on the tension side (point B, fig. 1(a)) when $\sigma_{xB} = S_{xT}$.

(3) Calculate the load P required to produce a stress $\sigma_{xB} = S_{xT}$.

(4) Knowing this load, calculate the corresponding stresses $\sigma_x$ and $\sigma_z$ in the immediate vicinity of point A.

(5) Plot this point in the tension-tension quadrant in figure 8. The tension quadrant is sufficient since we are interested in the case of equal compressive and tensile strengths; that is, $S_{xC} = S_{xT}$.

The point plotted in step (5) should fall inside the region bounded by the failure envelope to verify the conclusion for the case of equal strengths.

Following the preceding procedure yields: From equation (24) and $l/h = 20$,

$$P \approx \frac{bh}{30} S_{xT} \tag{33}$$

From the simple beam formula $\sigma_x = (1.5\, Pl/bh^2)$ (from fig. 8(a)) and P (from eq. (33)):

$$\sigma_{xA} = 0.957\, S_{xT}$$

Equation (25) at $2z/h = 0.95$ yields $\sigma_z bh/p \approx 25.4$. Using P from equation (33), we obtain

$$\sigma_{zA} = 0.85\, S_{xT}$$

The combined stress and the single stress are plotted as points A and B in figure 8. Point A in figure 8 is inside the failure envelope as was previously postulated. Therefore, the conclusion is verified for the equal strength case.

The $l/h$ at which $\sigma_{zA} = \sigma_{xA}$ is of interest. This ratio may be obtained readily following the previous procedure. The required equations are

$$\sigma_{xA} = -\frac{1.5\,P}{bh}\,\frac{l}{h} + \frac{1.30}{bh}P \tag{34}$$

$$\sigma_{zA} = -\frac{24}{bh}P \tag{35}$$

Equating these two equations yields

$$\left(\frac{l}{h}\right) \approx 17 \tag{36}$$

The interpretation of equation (36) is as follows:

$\left(\frac{l}{h}\right) > 17$ $\quad$ $\sigma_{xA}$ increases faster than $\sigma_{zA}$

$\left(\frac{l}{h}\right) = 17$ $\quad$ $\sigma_{xA}$ increases at the same rate as $\sigma_{zA}$

$\left(\frac{l}{h}\right) < 17$ $\quad$ $\sigma_{xA}$ increases slower than $\sigma_{zA}$

It is noted that as $l/h$ approaches one, $\sigma_{zA}$ will increase considerably faster than $\sigma_{xA}$ and produce local bearing failure under the load. At $l/h = 1$, $\sigma_{zA}/\sigma_{xA} \approx 8$ from equations (34) and (35).

The important conclusions from the previous discussion follow:

(1) Failure initiates on the tension side of a three-point-bend test specimen. This is the case for specimens made from materials with compressive strength equal to or greater than the tensile strength and with an $l/h$ greater than 17.

(2) The apparent flexural strength will be equal to or greater than the smaller of the simple strengths. If $S_{xT} < S_{xC}$, then $S_{xT} \leq$ flexural strength $< S_{xC}$.

## ADDITIONAL APPLICATIONS OF THE EQUATIONS AND GRAPHS

In addition to analyzing the three-point-bend test, the equations and graphs presented herein can be used in other ways. Some examples are briefly described. If the tensile modulus and the flexural modulus are known, the corresponding compressive modulus can be obtained from figure 4. The shear modulus can be obtained from figure 5. The neutral plane location is obtained from figure 2. If, in addition, the apparent flexural failure stress is known, the actual flexural failure stress may be obtained from figure 6.

The corresponding simple tensile strength and a lower bound on the compressive strength may be estimated by the use of equations (15a) and 16(a) and figure 7(a).

If a specimen fails in compression and the apparent flexural strength is known, the actual flexural strength can be obtained from equation 16(a). The corresponding simple compressive strength may be estimated using equation (16a), figures 7(a) and (b), and equation (32).

The actual and apparent flexural strengths can be estimated when the simple tensile or compressive strengths are known. The estimate may be obtained by following the procedures used in the previous section.

Equations (34) and (35) can be used to specify a loading rate ratio of $\sigma_{xA}/\sigma_{zA}$ (fig. 1). If the specimen is suspected to have failed by a combined stress state, including shear, then this condition can be checked by computing the stresses $\sigma_x$, $\sigma_z$, at that point and substituting in equation (32).

It is worth noting at this point that the procedures described herein apply to fiber composites as well. However, the data in the figures do not because the shear modulus was determined from equation (10) or (14), neither of which is valid for fiber composites. The procedures described previously are also applicable in sizing structural components.

## SOME COMMENTS ON INSTRUMENTING THE THREE-POINT-BEND TEST

The equations locating the neutral plane may be used in conjunction with figure 7(c) to locate strain gages for measuring the shear modulus using a three-point-bend test.

A direct determination of the location of the neutral plane can be obtained by measurement. This is accomplished by placing strain gages on the top and bottom surfaces of the specimen (near points A and B, fig. 1) along the x-direction. The gages should be placed at a distance $h/2$ away from the load to avoid local stress concentration effects.

Plotting the stresses predicted by equations (15a) and (16a) against the strains of the corresponding gages yields the required stress-strain curves which can be used to determine both the tensile and compressive moduli.

## SUMMARY OF RESULTS

Results obtained from analyses of three-point-bend tests for materials with different moduli in tension and compression are summarized in this section. The tensile-modulus to compressive-modulus ratio is referred to herein as the modular ratio (MR).

1. An analysis capability was generated. The capability can be used to analyze the test data or select test specimen geometry for three-point-bend tests.

2. The maximum flexural deflection is sensitive to MR. The simple beam formula underestimates the maximum deflection by 25 percent when the MR = 1.5 and overestimates it by 25 percent when MR = 0.5. The maximum bending deflection is insensitive to the length-to-depth ratio $l/h$ when $l/h$ is greater than 10.

3. The MR has significant influence on the flexural and shear moduli. Corrections of 35 and 25 percent, respectively, are needed for the simple beam formula predictions when MR = 0.5. But $l/h$ has negligible influence on the flexural modulus.

4. The flexural stress ratio (tensile to compressive stress) varies as the square root of MR. The maximum stress magnitude in tension (compression) occurs in the extreme fibers of the stiffer side. The correction to maximum tensile (compressive) stress can be as large as 25 percent compared to a material with equal moduli.

5. The local stress concentration in the vicinity of the load has negligible influence on the maximum flexural stress and deflection where $l/h$ equals 20 or greater. However, the maximum shear stress is increased by about 15 percent and occurs at about the one-fourth depth point from the top of the beam.

6. Failure will initiate on the tension side of a three-point-bend test specimen made from material with compressive strength equal to or greater than the tensile strength.

7. The equations and graphs can be readily used to extract data which are useful for design purposes and as a guide to instrumenting the test specimen.

Lewis Research Center,
National Aeronautics and Space Administration,
Cleveland, Ohio, November 8, 1973,
501-22.

## APPENDIX A

## SYMBOLS

| | |
|---|---|
| b | specimen, beam width |
| D | flexural stiffness |
| E | normal modulus |
| F | combined stress failure function |
| G | shear modulus |
| h | specimen thickness |
| $h_b$ | distance from neutral plane to bottom |
| $h_t$ | distance from neutral plane to top |
| $K_{xz\alpha\beta}$ | coefficient in combined stress failure function |
| $l$ | specimen length |
| M | resultant moment |
| P | applied load |
| S | simple strength |
| w | bending deflection |
| x | coordinate |
| z | coordinate |
| $\gamma$ | shear strain |
| $\epsilon$ | normal strain |
| $\nu$ | Poisson's ratio |
| $\sigma$ | normal stress |
| $\tau$ | shear stress |

Subscripts:

| | |
|---|---|
| b | bottom |
| C | compression |
| F | property obtained by simple beam formulas |
| ISO | isotropic material property |
| max | maximum value |
| T | tension |
| t | top |
| x | direction along x-axis |
| z | direction along z-axis |
| $\alpha$ | T or C, tension or compression |
| $\beta$ | T or C, tension or compression |

## APPENDIX B

## DERIVATIONS

### Basic Relations

The linear uniaxial stress-strain relations for a material with different moduli in tension and compression are given by

$$\sigma_T = \epsilon_T E_T \tag{B1}$$

$$\sigma_C = \epsilon_C E_C \tag{B2}$$

$$\tau = \gamma G \tag{B3}$$

The strain-displacement relations of interest in these derivations are given by (see fig. 1(d))

$$\epsilon = -z \frac{d^2 w}{dx^2} \tag{B4}$$

The force equilibrium equations of interest in these derivations are (figs. 1(a) and (b))

$$\frac{\partial \sigma_x}{\partial x} - \frac{\partial \tau_{xz}}{\partial z} = 0 \tag{B5}$$

where $0 \le x \le \ell$ and $h_b \le z \le h_t$,

$$\int_{-h_b}^{0} \sigma_T dz + \int_{0}^{h_t} \sigma_C dz = 0 \tag{B6}$$

where $0 \le x \le \ell$, and

$$M = b \int_{-h_b}^{0} z\sigma_T dz + b \int_{0}^{h_t} z\sigma_C dz \tag{B7}$$

where $0 \leq x \leq l$.

## Equation of the Neutral Plane

Using equation (B4) in equations (B1) and (B2), substituting the result in equation (B6), and carrying out the integration yield

$$\int_{-h_b}^{0} \sigma_T dz + \int_{0}^{h_t} \sigma_C dz = \frac{1}{2} E_T h_b^2 \frac{d^2w}{dx^2} - \frac{1}{2} E_C h_t^2 \frac{d^2w}{dx^2} = 0$$

From which follows

$$\left(\frac{h_t}{h_b}\right)^2 = \left(\frac{E_T}{E_C}\right) \tag{B8}$$

and

$$\left(\frac{h_t}{h_b}\right) = \left(\frac{E_T}{E_C}\right)^{1/2} \tag{B9}$$

Equation (B9) is the equation of the neutral plane. It can also be expressed in terms of h. Using the identity

$$h = h_t + h_b \tag{B10}$$

in equation (B9) and collecting terms yield

$$h_b = \frac{h}{1 + \left(\frac{E_T}{E_C}\right)^{1/2}} \tag{B11}$$

## Equation of Flexural Rigidity (Stiffness)

Using equation (B4) in equations (B1) and (B2), substituting the result in equation (B7), and carrying out the integration noting that $d^2w/dx^2$ is independent of $z$ yield

$$M = -b\left(\frac{1}{3}z^3E_T\Big|_{-h_b}^{0} + \frac{1}{3}z^3E_C\Big|_{0}^{h_t}\right)\frac{d^2w}{dx^2}$$

From which follows

$$M = -\frac{1}{3}b\left(h_b^3E_T + h_t^3E_C\right)\frac{d^2w}{dx^2} \tag{B12}$$

Let the coefficient of $d^2w/dx^2$ be D. Thus,

$$D = \frac{b}{3}\left(h_b^3E_T + h_t^3E_C\right) \tag{B13}$$

Equation (B13) is the flexural rigidity of a material with different moduli in tension and compression. Equation (B13) can be expressed in terms of either $h_b$ or $h_t$ and h through the use of equation (B8) or (B9) and equation (B10):

$$D = \frac{1}{3}bhh_b^2E_T = \frac{1}{3}bhh_t^2E_C \tag{B14}$$

The resultant moment in terms of D is

$$M = -D\frac{d^2w}{dx^2} \tag{B15}$$

## Stress Moment Relations

Multiplying by $z$ both sides of equation (B15) yields

$$Mz = -Dz \frac{d^2w}{dx^2}$$

and using equation (B4) results in

$$Mz = D\epsilon$$

Substituting equations (B1) and (B2) in the last equation and rearranging yield, respectively,

$$\sigma_T = Mz \frac{E_T}{D} \qquad 0 \le x \le l \qquad -h_b \le z \le 0 \tag{B16}$$

and

$$\sigma_C = Mz \frac{E_C}{D} \qquad 0 < x \le l \qquad 0 \le z \le h_t \tag{B17}$$

But in the region $0 \le x \le (l/2)$

$$M = -\frac{Px}{2} \tag{B18}$$

Using equation (B18) in equations (B16) and (B17) yields, respectively,

$$\sigma_T = -\frac{Pxz}{2D} E_T \qquad 0 \le x \le \frac{l}{2} \qquad -h_b \le z \le 0 \tag{B19}$$

$$\sigma_C = -\frac{Pxz}{2D} E_C \qquad 0 \le x \le \frac{l}{2} \qquad 0 \le z \le h_t \tag{B20}$$

The maximum tensile and compressive stresses are obtained by the following substitutions:

$x = \frac{l}{2}$ and $z = -h_b$ in equation (B19)

$x = \frac{l}{2}$ and $z = h_t$ in equation (B20)

The results are, respectively,

$$\sigma_{Tmax} = \frac{P\ell h_b}{4D} E_T$$

and

$$\sigma_{Cmax} = -\frac{P\ell h_t}{4D} E_C$$

Using the values of D from equation (B14), the last two equations become

$$\sigma_{Tmax} = \frac{3P}{4bh_b} \frac{\ell}{h} \tag{B21}$$

$$\sigma_{Cmax} = -\frac{3P}{4bh_t} \frac{\ell}{h} \tag{B22}$$

Letting $h_b = h_t = (h/2)$ in equations (B21) and/or (B22) results in

$$-\sigma_{Cmax} = \sigma_{Tmax} = \frac{3P\ell}{2h^2} \tag{B23}$$

which is the well known maximum stress formula. Equations (B21) and (B22) constitute the maximum stress formulas of interest in this investigation.

Shear Stress Applied Load Relation

From equation (B5) we have

$$\frac{\partial \sigma_x}{\partial x} - \frac{\partial \tau_{xz}}{\partial z} = 0 \tag{B5}$$

In the region $0 \le x \le (\ell/2)$ and $0 \le z \le h_t$, $\sigma_x$ is given by equation (B20). Substituting equation (B20) in equation (B5), carrying out the differentiation with respect to x, and integrating the result with respect to z yield

$$-\frac{Pz^2}{4D} E_C - \tau_{xz} + F(x) = 0$$

Applying the boundary condition at $z = h_t$ and $\tau_{xz} = 0$ yields

$$F(x) = \frac{Ph_t^2}{4D} E_C$$

Substituting this value of $F(x)$ in the previous equation and rearranging yield

$$\tau_{xz} = \frac{Ph_t^2 E_C}{4D}\left[1 - \left(\frac{z}{h_t}\right)^2\right] \tag{B24}$$

The maximum shear stress is obtained by letting $z = 0$ in equation (B24), using the value of $D$ from equation (B14), and using equation (B10). The result is

$$\tau_{xzmax} = \frac{3P}{4bh} \tag{B25}$$

Equation (B25) is the same as that of a material with equal moduli. However, the maximum value is <u>not</u> at the midplane of the specimen.

Carrying out the same procedure for the region $0 \le x \le (\ell/2)$ and $-h_b \le z \le 0$ yields

$$\tau_{xz} = \frac{Ph_b^2 E_t}{4D}\left[1 - \left(\frac{z}{h_b}\right)^2\right] \tag{B26}$$

But at $z = 0$ the shear stress predicted by equation (B26) must equal that of equation (B24). Carrying out the algebra and reducing the result yields

$$\left(\frac{h_t}{h_b}\right) = \left(\frac{E_T}{E_C}\right)^{1/2}$$

The last equation defines the plane of maximum shear stress. Note that this equation is the same as equation (B9), which is the equation for the neutral plane. Therefore, the neutral plane and plane of maximum shear stress coincide as is the case for materials with equal moduli.

## Maximum Flexural Deflection

The total energy stored in the beam is given by

$$U = 2b\int_0^{l/2} \frac{1}{2}\left\langle \int_{-h_b}^{0} (\sigma_T \epsilon_T + \tau\gamma)dz + \int_0^{h_t} (\sigma_C \epsilon_C + \tau\gamma)dz \right\rangle dx \qquad \text{(B27)}$$

Using the stress-strain relations (eqs. (B1) to (B3)) and the stress-force relations (eqs. (B19), (B20), and (B26)) in equation (B27) and carrying out the integrations and simplifying yield

$$U = \frac{P^2}{2}\left[\frac{l^3}{48D} + \frac{lb}{30GD^2}\left(E_T^2 h_b^5 + E_C^2 h_t^5\right)\right] \qquad \text{(B28)}$$

The midpoint deflection (maximum deflection) is obtained by differentiating equation (B28) with respect to P (Castigleano's first theorem). The result after simplification is

$$w_{max} = w_{l/2} = \frac{Pl^3}{48D}\left[1 + \frac{1.6\, bh_b^2 h E_T^2}{GD}\left(\frac{h_b}{l}\right)^2\right] \qquad \text{(B29)}$$

When $E_T = E_C$, $h_t = h_b = (h/2)$, equation (B29) reduces to

$$w_{max} = \frac{Pl^3}{4bh^3E}\left[1 + 1.2\left(\frac{E}{G}\right)\left(\frac{h}{l}\right)^2\right] \qquad \text{(B30)}$$

Equation (B30) is the simple beam formula when the shear contribution is included.

The shear contribution to the maximum deflection may be limited to specified values by adjusting the ($l$/h) ratio in equation (B30). For example, if the shear contribution is to be limited to 1 percent or less, then $l$/h is

$$\left(\frac{l}{h}\right) > \left(\frac{120E}{G}\right)^{1/2}$$

For isotropic materials $E/G \approx 3$ and $l/h > 19$. However, for advanced fiber composites for which equation (B30) applies, $E/G \approx 30$ and $l/h > 60$, which is considerable. This procedure can be used to size components from these materials.

## Relations Between Shear, Tensile, and Compressive Moduli

Relations for G and $E_T$ and $E_C$ are obtained in the following manner: Refer to figure 9(a). For the stress state shown, the strain energy stored in a unit-volume-element is

$$U = \frac{1}{2}\epsilon_T\sigma_T + \nu_C\epsilon_C\sigma_T + \frac{1}{2}\epsilon_C\sigma_C$$

Using equations (B1) and (B2) yields

$$U = \frac{1}{2E_T}\sigma_T^2 + \frac{\nu_C}{E_C}\sigma_C\sigma_T + \frac{1}{2E_C}\sigma_C^2 \tag{B31}$$

in terms of stresses only.

For the stress state in figure 9(b) the energy stored in a unit-volume-element in terms of stresses only is

$$U = \frac{1}{2E_C}\sigma_C^2 + \frac{\nu_T}{E_T}\sigma_T\sigma_C + \frac{1}{2E_T}\sigma_T^2 \tag{B32}$$

Assuming no energy loss during the stressing-straining process, the energy is the same in both cases. Subtracting equation (B31) from equation (B32), we obtain

$$\frac{\nu_T}{E_T} = \frac{\nu_C}{E_C} \tag{B33}$$

If in figures 9(a) or (b) we let the magnitude of $\sigma_C = \sigma_T$, we have a case of pure shear that can be expressed as

$$\tau = |\sigma_C| = \sigma_T \tag{B34}$$

The energy stored in a unit-volume-element for the case of pure shear is given by

$$U = \frac{1}{2}\gamma\tau = \frac{1}{2G}\tau^2 \tag{B35}$$

But the energy in equation (B35) is equal to that of equation (B31) or equation (B32) since it is produced by the equivalent final stress states. Equating equation (B35) to, say, equation (B31), we obtain

$$\frac{1}{2G}\tau^2 = \frac{1}{2E_T}\sigma_T^2 + \frac{\nu_C}{E_C}\sigma_C\sigma_T + \frac{1}{2E_C}\sigma_C^2 \tag{B36}$$

Using equations (B33) and (B34) in equation (B36), we obtain, after simplification,

$$G = \frac{E_T}{1 + 2\nu_T + \left(\frac{E_T}{E_C}\right)} \tag{B37}$$

Equation (B37) reduces to the well known case for $E_C = E_T$ as can be verified by inspection.

When $E_T$, $\nu_T$, and G are known from independent tests and not from the relation $E = 2(1 + \nu)G$, then the compressive modulus $E_C$ can be computed from equation (B37). The result is

$$E_C = \frac{E_T}{\frac{E_T}{G} - (1 + 2\nu_T)}$$

Equation (B38) indicates that a material with $E_T = G(1 + 2\nu_T)$ is incompressible.

We note here, that analogous derivations leading to relation of equation (B37) are presented in reference 7.

## Approximate Equation for the Flexural Modulus

Assume that the flexural modulus may be approximated by the average extensional modulus through the beam thickness. In equation form it is

$$E_F \approx \frac{1}{h}(h_b E_T + h_t E_C) = \frac{h_b E_T}{h}\left(1 + \frac{h_t}{h_b}\frac{E_C}{E_T}\right) \tag{B39}$$

Using the relation $E_C/E_T = (h_b/h_t)^2$ (eq. (B8)) in equation (B39) and simplifying yields

$$E_F \approx \left(\frac{h_b}{h_t}\right) E_T = \sqrt{E_T E_C} \tag{B40}$$

as an approximate equation for determining the flexural modulus.

## REFERENCES


1. Heat, R. D.; and Norman, R. H.: Flexural Testing of Plastics. Plastics Institute, London, 1969.

2. Yamamoto, C. A.: Evaluation Techniques for Simple Mechanical Property Tests on Composite Materials. Advanced Techniques for Material Investigation and Fabrication. Western Periodicals Co., 1968, paper I-2-3.

3. Mowforth, E.: Non-Linear Bending of a Random-Fibre Laminate. Composites, vol. 1, no. 2, Dec. 1969, pp. 76-79.

4. Ogorkiewicz, R. M.; and Mucc, P. E. R.: Testing of Fibre-Plastics Composites in Three-Point Bending. Composites, vol. 2, no. 3, Sept. 1971, pp. 139-145.

5. Timoshenko, S.; and Goodier, J. N.: Theory of Elasticity. Second ed., McGraw-Hill Book Co., Inc., 1951.

6. Chamis, Christos C.: Failure Criteria for Filamentary Composites. NASA TN D-5367, 1969.

7. Noyes, Joseph V.; and Jones, B. H.: Crazing and Yielding of Reinforced Composites. McDonnell-Douglas Co. (AFML-TR-68-51) Mar. 1968.

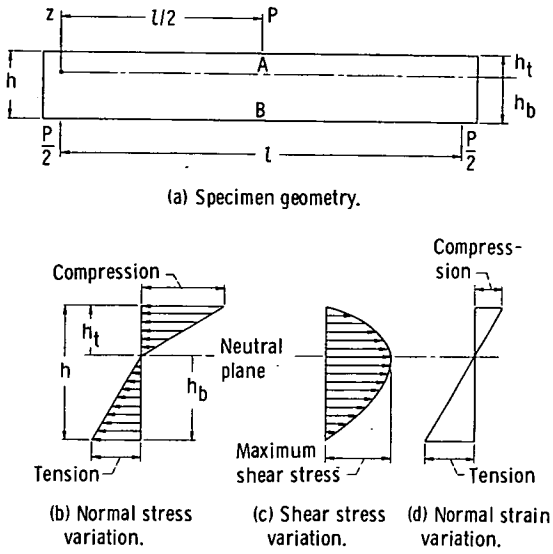


Figure 1. - Schematic of geometry and stress variations of three-point-bending test specimen from material with unequal tensile and compressive properties.

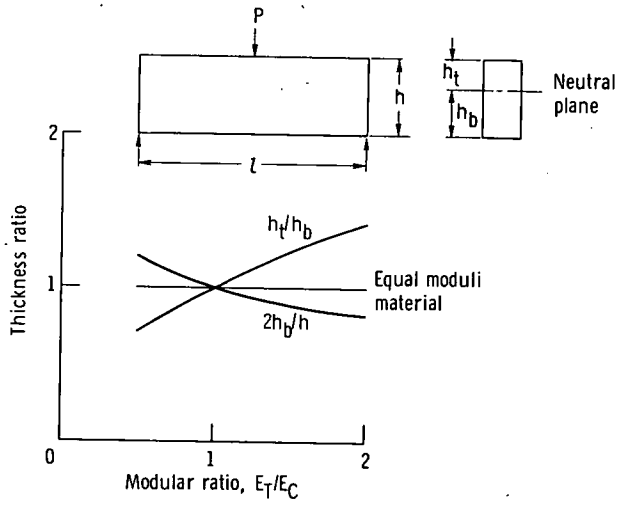


Figure 2. - Effect of modular ratio on shift of neutral plane for three-point bending.

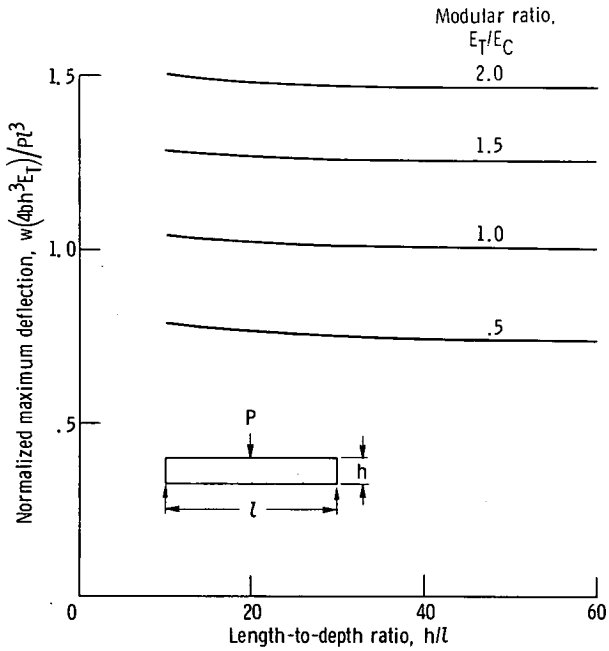


Figure 3. - Maximum deflection of three-point-bending beam made from material with unequal tensile and compression. Moduli maximum deflection normalized with respect to that of equal moduli.

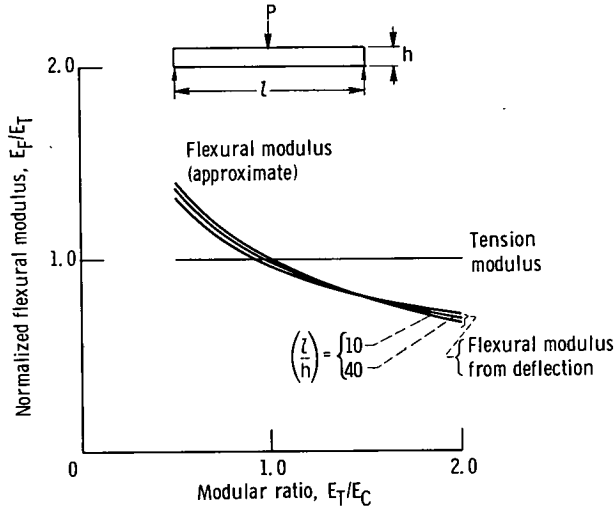


Figure 4. - Effect of modular ratio of flexural modulus for three-point bending.

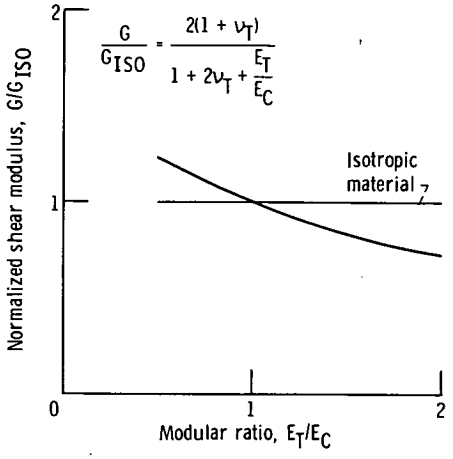


Figure 5. - Shear modulus of material having different values for tension and compression moduli; Poisson's ratio = 0.4.

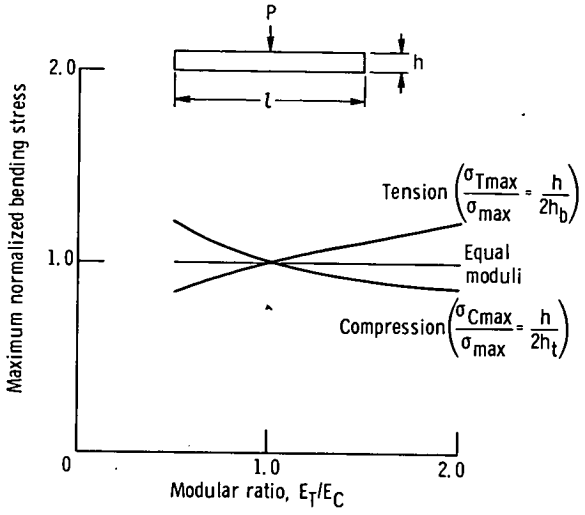


Figure 6. - Effect of modular ratio on maximum bending stress for three-point bending ($\ell/b = 40$).

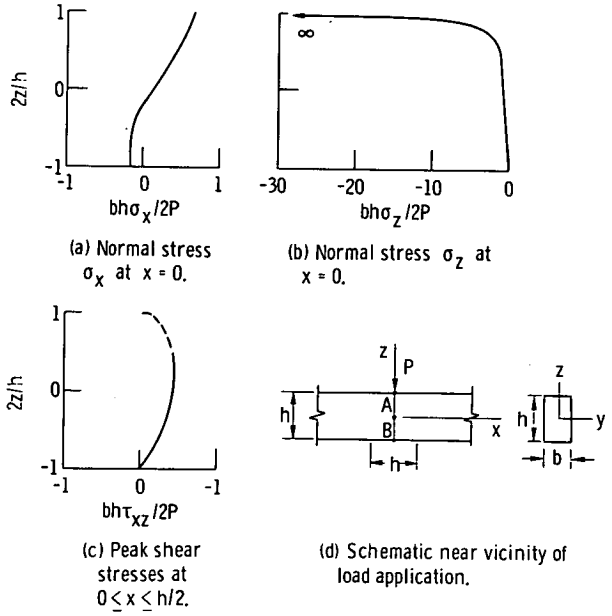


(a) Normal stress $\sigma_x$ at $x = 0$.

(b) Normal stress $\sigma_z$ at $x = 0$.

(c) Peak shear stresses at $0 \leq x \leq h/2$.

(d) Schematic near vicinity of load application.

Figure 7. - Stress variation in vicinity of applied load for modular ratio, $E_T/E_C$, 1. (For geometry notation part (d) this figure.)

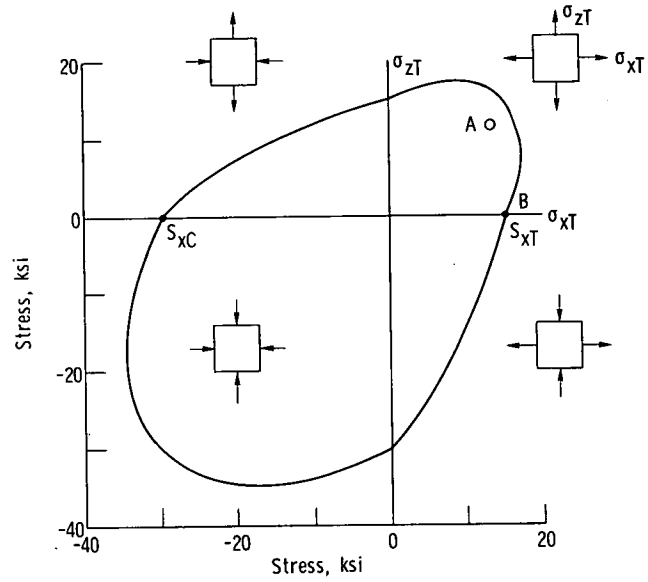


Figure 8. - Failure envelope for typical epoxy resin in biaxial stress field.

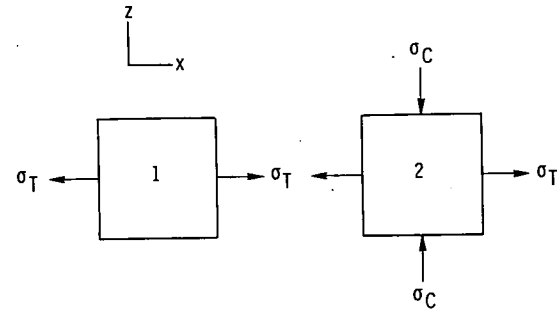


(a) Tension then compression.

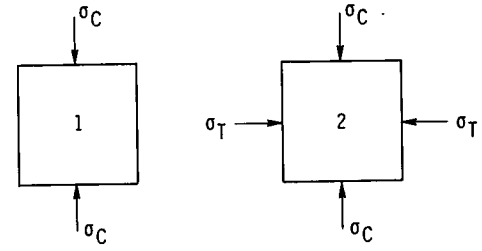


(b) Compression then tension.

Figure 9. - Stress application for determining relations between shear, tensile, and compressive moduli.

NATIONAL AERONAUTICS AND SPACE ADMINISTRATION
WASHINGTON, D.C. 20546

OFFICIAL BUSINESS
PENALTY FOR PRIVATE USE $300

SPECIAL FOURTH-CLASS RATE
BOOK

POSTAGE AND FEES PAID
NATIONAL AERONAUTICS AND
SPACE ADMINISTRATION
451

U.S.MAIL

POSTMASTER: If Undeliverable (Section 158 Postal Manual) Do Not Return

*"The aeronautical and space activities of the United States shall be conducted so as to contribute . . . to the expansion of human knowledge of phenomena in the atmosphere and space. The Administration shall provide for the widest practicable and appropriate dissemination of information concerning its activities and the results thereof."*

—NATIONAL AERONAUTICS AND SPACE ACT OF 1958

# NASA SCIENTIFIC AND TECHNICAL PUBLICATIONS

TECHNICAL REPORTS: Scientific and technical information considered important, complete, and a lasting contribution to existing knowledge.

TECHNICAL NOTES: Information less broad in scope but nevertheless of importance as a contribution to existing knowledge.

TECHNICAL MEMORANDUMS: Information receiving limited distribution because of preliminary data, security classification, or other reasons. Also includes conference proceedings with either limited or unlimited distribution.

CONTRACTOR REPORTS: Scientific and technical information generated under a NASA contract or grant and considered an important contribution to existing knowledge.

TECHNICAL TRANSLATIONS: Information published in a foreign language considered to merit NASA distribution in English.

SPECIAL PUBLICATIONS: Information derived from or of value to NASA activities. Publications include final reports of major projects, monographs, data compilations, handbooks, sourcebooks, and special bibliographies.

TECHNOLOGY UTILIZATION PUBLICATIONS: Information on technology used by NASA that may be of particular interest in commercial and other non-aerospace applications. Publications include Tech Briefs, Technology Utilization Reports and Technology Surveys.

***Details on the availability of these publications may be obtained from:***

**SCIENTIFIC AND TECHNICAL INFORMATION OFFICE**

**NATIONAL AERONAUTICS AND SPACE ADMINISTRATION**

**Washington, D.C. 20546**